International Journal of Statistics and Applied Mathematics

ISSN: 2456-1452
NAAS Rating (2025): 4.49
Maths 2025; 10(9): 01-13

https://www.mathsjournal.com
Received: 03-07-2025
Accepted: 04-08-2025

Raja Sekhara Reddy K
Department of Mathematics, Government First Grade College, Gauribidanur, Karnataka, India

DT Hanumantha Reddy
Department of Mathematics, Government College for Women, Chintamani, Karnataka, India

Corresponding Author:
K Raja Sekhara Reddy
Department of Mathematics, Government First Grade College, Gauribidanur, Karnataka, India

Effect of asymmetric slip and Newtonian cooling on MHD, radiation, convective and heat and mass transfer flow of ethylene glycol based copper (CU) nanofluid in vertical channel with variable properties

Raja Sekhara Reddy K and Hanumantha Reddy DT

DOI: https://www.doi.org/10.22271/maths.2025.v10.i9a.2156

Abstract
In this examination, the study of thermal radiation, dissipation, non-uniform heat sources on hydro magnetic rotating, convective heat and mass transfer flow of Eg based Cu nanofluid limited in a vertical channel with asymmetric slips and convective boundary conditions in the course of a porous medium. After evaluating the governing equations numerically, we find that increase in asymmetric slips (αo, $\alpha 1$) outcome in an augmentation in *u* (velocity), θ(temperature) and C (nano concentration) at $\eta=0$. An upsurge in Biot numbers (Bio, Bi1) augments u, θ and C at $\eta=\pm 1$. Stress, Nusselt (Nu) and Sherwood (Sh) numbers enhance with increase in Bio and depreciate with higher values of Bi1.

Keywords: Heat and mass transfer, EG based cu nanofluid, vertical channel, thermal radiation, dissipation, non-uniform heat source, asymmetric slip, newtonian cooling, activation energy

Introduction
The transfer of warmth and mass difficulties are predicted to have increasingly notable usages in the late decades due to their widespread use and value in technological areas. Over the decades, many scholars have conducted significant investigations in *MHD*, natural and induced convection, heat and mass streams, taking into account the effects of chemical processes as well as Soret and Dufour impacts. Despite claiming that the journals on the issue are exhaustive, an effort is made below to highlight the key studies, while confining the references to the context and parameters of this study. Anghel *et al.* [8], and Muralidhar [36] and Raju *et al.* [43] were investigated the Dufour and Soret effects on a free convection boundary layer with heat and mass transfer flow across a vertical surface buried in a porous material using a regular perturbation technique.

Nanoparticles with high thermal conductivity can be elements the oxides, the carbides, or nitrides, while the base fluid can be water, kerosene, motor oil, toluene, ethylene, or tri-ethylene glycol, depending on the procedure utilized. Several authors have been studied and experimental examined by Choi and Eastman [15], Choi [16], Choi *et al.* [17], Das *et al.* [18] were probably the first to employ a mixture of nanoparticles and base fluid that such fluids were designated as *nano-fluids*.

Thermal radiation is the means whereby a warm surface emits energy in all instructions in the outline of electromagnetic waves that arrangements in alluring and exciting waves. Mondal *et al.* [35], Prakash *et al.* [42], Umamaheswar *et al.* [48], and Vedavathi *et al.* [50], Alam and Ahammad [5] and Kumar *et al.* [30] have investigated the influence of radiation on heat transport difficulties with exothermic chemical processes and heat generation. A research investigation of heat radiation on free convection flow has a variety of use cases, including high-speed flights, space vehicle reentry, and thermal power plants.

The natural conduction of air within conduits is the focus of extensive investigation in the past few decades due to its technical uses, including electronic cooling systems, nuclear reactors, and exchanges of heat.

The vertical channel is a commonly used set up in heating tools, such as solar power collectors and cooling devices for digital and micro-digital equipment by Gill and Casal [23], Ostrach [40], Cebeci *et al.* [13], Datta and Jana [19], Barletta [10], and Barletta *et al.* [11].
Non-Darcy effects on transpiration in porous surfaces have received a lot of focus lately due to testing done with different blends of particles and water wrapping an array of dealing with variables, that reveal that data collected for platforms outside of a glass liquid at tiny Rayleigh parameters conflict with theorems depending within the Darcy flow model. This discrepancy in radiation transfer findings was quite thoroughly explored in Cheng *et al.* [14], many a few more.
The condition with Newton's law of thermodynamics occurs in what are often known as conjugate convective flows, in which heat is given to the flowing fluid via a bounding surface with a limited heat capacity. Several researchers, including Merkin [34], Lesnic *et al.* [32], Rao and Reddy [45], have examined a different but still applicable guiding system for convective flow across boundaries close to a straight exterior. In these studies, it was thought that flow was started by Newtonian warming from the boundary, meaning that the heat transfer from the surface was identical at the personal surface temperature.
The no-slip boundary condition (the assumption that a liquid clings to a solid border) is commonly used in flow issues involving viscous fluids. Slip may occur on the boundary when the fluid is particulate, as in emulsions, suspensions, foams, and polymer solutions. Many scholars have examined slip flows in different flow configurations. Abbasbandy and Shirzadi [1], Rashidi *et al.* [44], Hayat *et al.* [24], Hayat *et al.* [26-28], Ellahi *et al.* [21], Awais *et al.* [5], Adetayo *et al.* [4], Anghel and Takhar [8], Falade [22] use the homotopy analysis approach to create asymmetric Navier slips.
In chemistry and physics, activation energy is the smallest quantity of energy necessary for a molecule to undergo a chemical reaction. A reaction's activation energy (Ea) can be represented as joules per mole (J/mol), kilojoules per mole (kJ/mol), or kilocalories per mole. Arrhenius [7], a Swedish scientist, coined the word "activation energy" in 1889. Several writers have studied the energy of activation, including Abu-Nada *et al.* [2] and Abu-Nada and Eiyad [3], Tiwari [47], Kathyani and Subramanyam [28], Narayana and Ramakrishna [39], Nagasasikala [39], and Devasena [20], Lalramngaihzuali and Rao [31], and Kumar *et al.* [29], who addressed the effects of energy of activation on the hydromagnetic convective
In most of the studies the viscosity of the fluid was assumed to be constant, When the effects of variable viscosity is taken into account, the flow characteristics are significantly changed compared to the constant property case. Ali (2006) was briefly discussed the effect of variable viscosity on mixed convection heat transfer along a vertical moving surface are studied by Abu-Nada *et al.* [2] and Abu-Nada *et al.* [3], Vajravelu *et al.* [49], Makinde [34], Satya Narayana and Ramakrishna [45], Nagasasikala [39], Devasena [20].
Asymmetric slip and congested boundaries that characterize the *MHD* non-darcy turbulent mass and thermal flow of a Cu nanofluid based on ethylene in a vertical channel with asymmetrical warmth sources. Using Galerkine Finite element method with quadratic interpolation functions the non-linear, coupled equations governing the flow, heat and mass transfer have been executed. The velocity, temperature & nanoconcentration, Stress, Nusselt and Sherwood numbers have exhibited through graphs and tables.

Formulation of the Problem
The fluid consists of an ethylene glycol base fluid and tiny copper nanoparticles in a vertical porous tube with heat radiation. A homogeneous magnetic field with strength Ho is applied normal to the plate. Because of the fully matured assumption, the flow variables are just y-dependent. Fig – 2.1 depicts both the problem under examination and a coordinate system.

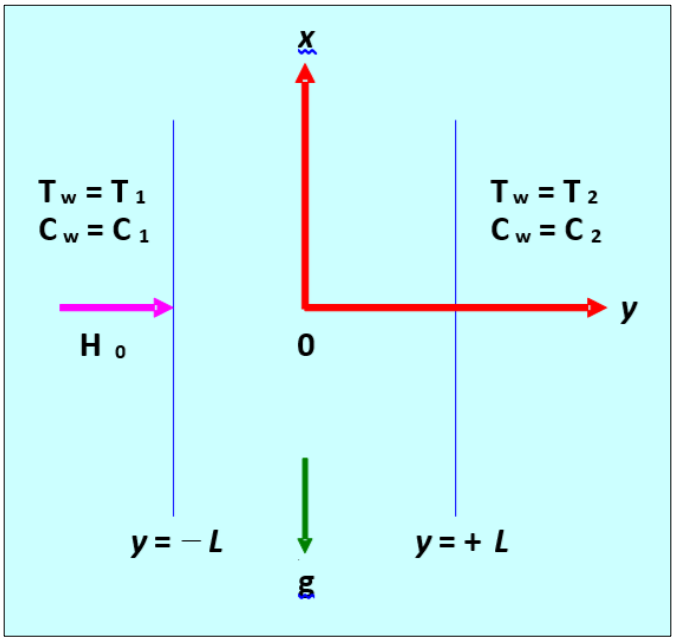

Under Rosseland approximation can be written in dimensional form as :

$$\frac{\partial v}{\partial y} = 0, \tag{1}$$

$$-\rho_{nf} v_o \frac{\partial u}{\partial y} = -\frac{\partial P}{\partial y} + \frac{\partial}{\partial y}[\mu_{nf} \frac{\partial u}{\partial y}] + (\rho\beta_T)_{nf} g(T - T_o) - \left| \begin{array}{l} -\sigma_{nf} \mu_e^2 \, \mathrm{H}_o^2(u) - (\frac{\mu_{nf}}{k_p})u - (\frac{C_b}{\sqrt{k_p}})\mathrm{u}^2 \end{array} \right. \quad (2)$$

$$-v_o \frac{\partial T}{\partial y} = \frac{k_{nf}}{(\rho C_p)_{nf}} \frac{\partial^2 T}{\partial y^2} - \frac{1}{(\rho C_p)_{nf}} \frac{\partial (q_R)}{\partial y} + \frac{1}{(\rho C_p)_{nf}} (A_{11}^{'}(T_f - T_o)u + B_{11}^{'}(T - T_o))$$

$$+2\mu_{nf}[(\frac{\partial u}{\partial y})^2 + (\frac{\partial w}{\partial y})^2] + \sigma_{nf} \mu_e^2 H_o^2(u^2) + \mathrm{Q}_1^{'}(C - C_o)$$

$$-v_o \frac{\partial C}{\partial y} = D_B \frac{\partial^2 C}{\partial y^2} + D_T \frac{\partial^2 T}{\partial y^2} - kc(C - C_o)(\frac{T}{T_o})^n Exp(-\frac{E_a}{KT}) \quad (3)$$

The boundary conditions [42, 43] are as follows

$$\begin{aligned} u(-L) &= \alpha_o^{'} \frac{\partial u}{\partial y} \quad , k_{nf} \frac{\partial T}{\partial y} = \gamma_o (T - T_o), C = C_o \; on \;\; y = -L \\ u(+L) &= -\alpha_1^{'} \frac{\partial u}{\partial y} \; , \; k_{nf} \frac{\partial T}{\partial y} = \gamma_1 (T - T_f), C = C_f \;\; on \;\; y = +L \end{aligned} \quad (4)$$

where ($\alpha_o^{'}$, $\alpha_1^{'}$) -Navier slip, μ_f -viscosity fluid, u-axial velocity, P-fluid pressure, ρ_f is the density of the nanoparticle, v_o=channel porosity, Cp-constant pressure,(T,C)are the nanofluid temperature, concentration and kf is the thermal conductivity of the material respectively,(T_o,T_1)-temperature,(C_o,C_1)Concentration and $\gamma_{o,1}$-Newtonian cooling. D_B is the molecular diffusivity, are the effective thermal expansion of the nanofluid which are given by.

$$\begin{aligned} &\mu_{nf} = \mu_f / (1-\varphi)^{2.5} \qquad \alpha_{nf} = \frac{k_{nf}}{(\rho C_p)_{nf}} \qquad \rho_{nf} = (1-\varphi)\rho_f + \varphi\rho_s \\ &(\rho C_p)_{nf} = (1-\varphi)(\rho C_P)_f + \varphi(\rho C_P)_s \qquad (\rho\beta)_{nf} = (1-\varphi)(\rho\beta)_f + \varphi(\rho\beta)_s \\ &k_{nf} = \frac{k_f(k_s + 2k_f - 2\varphi(k_f - k_s)}{(k_s + 2k_f + 2\varphi(k_f - k_s)}, \sigma_{nf} = (\sigma_f + \frac{3(\sigma_f - \sigma_s)\phi}{(\sigma_s + 2\sigma_f)}), \end{aligned} \quad (5)$$

where the addendums nf, f and s address the thermo actual properties of the nanofluid, base liquid and the nanosolid particles individually and □ is the strong volume part of the nanoparticles. The thermo actual properties of the nanofluid are given in Table 2.1.

The thermo physical properties of the nanofluids are given in Table 2.1 (See *Ozotop and Abu-Nada* [41]).

Table 2.1: Physical Properties of nanofluids

Physical properties	Fluid phase (Ethylene Glycol)	Cu nanofluid
C_p(j/kg K)	2430	385
ρ(kg m^3)	1115	8933
k(W/m K)	0.253	401
βx10^{-5} 1/k)	5.7	1.67
σ	10.7	5.96

By using Rosseland approximation for radiative heat flux, qr is simplified as

$$q_r = -\frac{4\sigma^{\bullet}}{3\beta_R} \frac{\partial T'^4}{\partial y} \quad (6)$$

This is done by expanding T'^4 in a Taylor series about top wall temperature *Ti* as follows:

$$T'^4 \; \square \; T_o^4 + 3T_o^3(T - T_o) + 6T_o^2(T - T_o)^2 + - - - - \quad (7)$$

Neglecting higher order terms in the above equation beyond the first order in $(T - T_o)$, wae get

$$T'^4 \cong 4T_o^3 T - 3T_o^4 \quad (8)$$

In view of the equations (2.6) and (2.8),equation(2.2) becomes

$$-v_o\frac{\partial T}{\partial y}=\frac{k_{nf}}{(\rho C_p)_{nf}}\frac{\partial^2 T}{\partial y^2}+\frac{1}{(\rho C_p)_{nf}}\frac{16\sigma^* T_o^3}{3\beta_R}\frac{\partial^2 T}{\partial y^2}+\frac{1}{(\rho C_p)_{nf}}(A_{11}^{'}(T_f-T_o)u+B_{11}^{'}(T-T_o))$$
$$+2\mu_{nf}[(\frac{\partial u}{\partial y})^2+(\frac{\partial w}{\partial y})^2]+\sigma_{nf}\mu_e^2H_o^2(u^2)+Q_1^{'}(C-C_o) \quad (9)$$

and solution of eq (1) becomes

$v=-v_0$ (10)

Introducing the following dimensionless variables:

$$y'=\frac{y}{L},\ u'=\frac{u}{U},\ p'=\frac{p}{\rho_f U^2},\ \theta=\frac{T-T_0}{T_f-T_0},\ C=\frac{C-C_0}{C_f-C_0} \quad (11)$$

appropriate boundary conditions of ordinary differential equations are

$$(\frac{\partial^2 u}{\partial y^2}-B\frac{\partial u}{\partial y}\frac{\partial \theta}{\partial y})+[1+A_2S\frac{\partial u}{\partial y}A_1A_3G(\theta)-A_6M^2(u)-\Delta(u^2)]e^{B\theta}=0 \quad (12)$$

$$(A_5+\frac{4Rd}{3})\frac{\partial^2\theta}{\partial y^2}+(A_4S\,\Pr)\frac{\partial\theta}{\partial y}+A_{11}u+B_{11}\theta+Ec\,\Pr[e^{-B\theta}(\frac{\partial u}{\partial y})^2+A_6M^2(u^2)]=0$$

$$\frac{\partial^2 C}{\partial y^2}+(A_4SSc)\frac{\partial C}{\partial y}+ScSr(\frac{\partial^2 C}{\partial y^2})-\gamma C(1+n\delta\theta)\,E\,xp(-\frac{E_1}{1+\delta\theta})=0 \quad (13)$$

The transformed boundary conditions (3) reduce to

$$u(-1)=\alpha_0\frac{\partial u}{\partial y}(-1),u(+1)=-\alpha_1\frac{\partial u}{\partial y}(+1),$$
$$\frac{\partial\theta}{\partial y}(-1)=(\frac{Bi_o}{A_5})\theta(-1),\frac{\partial\theta}{\partial y}(+1)=-(\frac{Bi_1}{A_5})\theta(+1) \quad (14)$$

how good u defines the undefined flow rate, $\alpha_{0,1}$ are the undefined slip factors at the barrier, S is the fluid suction/injection factor due to duct pores, and Bi0,1 are the Biot coefficients.

$G=\frac{\beta g(T_f-T_o)L^2}{\mu_f U}$ (Grashof number), $S=\frac{v_0 L}{U}$ (Suction parameter)

$M=\frac{\sigma\mu_e^2H_0^2L^2}{\rho_f U\mu_f}$ (Magnetic parameter), $\Delta=\frac{C_bUL}{\sqrt{k_p}}$ (Forchheimer parameter)

$A_{11}=\frac{A_{11}^{'}L^2}{\rho_f C_p}$ (Space dependent heat source), $B_{11}=\frac{B_{11}^{'}L^2}{\rho_f C_p}$ (Temperature dependent heat source), $Rd=\frac{4\sigma^{\bullet}T_\infty^3}{\beta_R k_f}$ (Radiation parameter), $\Pr=\frac{\mu_f C_p}{k_f}$ (Prandtl number),

$Ec=\frac{U^2}{C_p(T_f-T_o)}$ (Eckert parameter), $Sc=\frac{\nu_f}{D_B}$ is the Schmidt number, $Sr=\frac{D_T(C_f-C_o)}{T_m(T_f-T_0)}$ is the Soret parameter,

$\theta_w = \frac{T_f}{T_0}, \delta = \theta_w - 1$ is the temperature difference ratio, $E_1 = \frac{E_a}{KT_0}$ is the Activation energy parameter

$$A_1 = (1-\varphi)^{2.5}\ ,\ A_2 = 1-\varphi+\varphi(\frac{\rho_s}{\rho_f})\ \ A_3 = 1-\varphi+\varphi((\frac{(\rho\beta)_s}{(\rho\beta)_f}), A_4 = 1-\varphi+\varphi\frac{(\rho C_P)_s}{(\rho C_P)_f}$$

$$A_5 = \frac{k_{nf}}{k_f}, A_6 = (1+\frac{3(1-\sigma)\phi}{(\sigma+2)}), \sigma = \frac{\sigma_s}{\sigma_f}$$

The limiting case $\alpha_{0,1} \to \infty$ parallels to the seamless lubricated plate surface.

3. Finite Element Analysis

Using quadratic polynomial estimation functions, a study of finite elements is performed along the axial distance across the vertical channel. For various changes in the controlling parameters, the behavior of the pressure, temperature, and velocity profiles is being computationally studied. Throughout the finite element analysis, the Galerkin method was used in the variational formulation of each element to get the global linked matrices for the degrees of freedom, quantity, and velocity. Select any element e_k and assign the values of u_k, and C to it (u_k, θ_k, and C_k).

The error residuals are defined as

$$E_u^k = \frac{d}{dy}\left(\frac{du^k}{dy}\right) + A_1A_3G(\theta^k) + Su^k + A_1 - A_1A_6M^2(u^k) - \Delta(u^k)^2 \tag{15}$$

$$E^k{}_\theta = \frac{A_5}{\Pr}\frac{d}{dy}\left(\frac{d\theta^k}{dy}\right) - S\theta^k A_4 u^k + A_{11}u^k + B_{11}\theta^k + Ec[(\frac{du^k}{dy})^2] + \\ + \mathrm{EcM^2A_6}(u^k)^2 \tag{16}$$

$$E^k{}_C = \frac{d}{dy}\left(\frac{dC^k}{dy}\right) - SSc(u^k) + ScSr\frac{d}{dy}\left(\frac{d\theta^k}{dy}\right) - \\ -\gamma Sc(C^k)(1+n\delta\theta^k)Exp(-\frac{E_1}{1+\delta\theta^k}) \tag{17}$$

The linear combinations in terms of respective local nodal values are

$$u^k = u_1^k\psi_1^k + u_2^k\psi_1^k + u_3^k\psi_3^k\ , \theta^k = \theta_1^k\psi_1^k + \theta_2^k\psi_2^k + \theta_3^k\psi_3^k\ , C^k = C_1^k\psi_1^k + C_2^k\psi_2^k + C_3^k\psi_3^k \tag{18}$$

where ψ_1^k , ψ_2^k … etc are Lagrange's quadratic polynomials.

The partial differential equations (3.1)–(3.2) are transformed into matrix form of solutions using Galarkin's approach, yielding 3x3 local stiffness matrices. Through the use of inter element continuity, a state of equilibrium, and a substitution of nationwide nodal values, all of these local matrices are integrated into a global matrix. The global matrices that were produced were then solved iteratively until integration or $|u_{i+1}\text{-}u_i| < 10^{-6}$, was achieved.

4. Comparison

In the absence of convection (G=0), heat sources (A11=0=B11), variable viscosity (B=0), activation energy (E1=0), δ=0 the results are in good agreement with *Falade John* [22]

Para-meter	*Falade John* [22]				Present results			
	τ(-1)	τ(+1)	Nu(-1)	Nu(+1)	τ(-1)	τ(+1)	Nu(-1)	Nu(+1)
M	1.07612	0.93072	0.264868	0.678584	1.07616	0.93074	0.264869	0.678587
	1.06352	0.91948	0.264384	0.677301	1.06355	0.91949	0.264385	0.677307
	1.03616	0.89501	0.263057	0.673813	1.03614	0.89502	0.263056	0.673819
S	1.07611	0.93072	0.264870	0.678586	1.07613	0.93073	0.264872	0.678589
	1.14285	0.87496	0.261245	0.677394	1.14286	0.87498	0.261245	0.677397
	1.20148	0.81987	0.255948	0.661667	1.20149	0.81988	0.255948	0.661664
Ec	…	…	0.332844	0.858343	…	…	0.332847	0.858344
			0.399164	1.010345			0.399166	1.010346
			0.448915	1.011167			0.448917	1.011166
Pr	…	…	0.026506	0.067915	…	…	0.026507	0.067916
			0.069255	0.177434			0.069256	0.177435
			0.119911	0.286912			0.119913	0.286913
αo	1.07613	0.93073	0.264871	0.678585	1.07614	0.93074	0.264872	0.678586
	0.97714	1.01155	0.311924	0.807821	0.97715	1.01156	0.311925	0.807822
	0.89847	1.07582	0.349923	0.912144	0.89848	1.07583	0.349924	0.912145
α1`	1.12742	0.88861	0.265258	0.752469	1.12749	0.88869	0.265259	0.752466
	1.20334	0.82628	0.340627	0.862844	1.20336	0.82629	0.340626	0.862845
	1..26932	0.77213	0.380441	0.959778	1..26929	0.77214	0.380442	0.959779
Bio	…	...	0.264866	0.678584	…	…	0.264863	0.678586
			0.541767	0.955267			0.541769	0.955269
			1.016422	2.205502			1.016424	2.205509
Bi1	…	…	0.118607	0.532444	…	…	0.118605	0.532446
			0.045989	0.459881			0.045987	0.459882
			0.015638	0.429554			0.015634	0.429558

5. Results and Discussion

An investigation of the effects of changing viscosity, thermal radiation, asymmetric slip, and non-uniform warmth source on the mass transfer and convective heat flow of an EG-based nanofluid in an upward channel under Newtonian cooling is being attempted in this work. Different parametric modifications have been considered with regard to Temperature (θ), Velocity (u), and Nano concentration(C).

1. Figs.2a-2c are Grashof number (G) & magnetic parameter (M). An increase in thermal buoyancy parameter G leads to an enhancement in the magnitude of nanofluid velocity field in Ethylene based Cu nanofluid. *u* increases in the flow region(-1.0,0) and decreases in the region (0,1.0) with increasing M. An increase in G increases θ & C at η=0.
2. Figs.3a-3c are Inverse Darcy parameter K (=D^{-1}) and Forchheimer parameter (Δ). *u* distribution decreases at -1.0,1.0 with increasing K(=D^{-1}) in Eg-Cu nanofluid. Δ on *u* shows, an effect of inaction and boundary diminishes *u* and enhance θ in Eg based Cu-nanofluid. θ distribution and C decays along upsurges standards of K as a findings of fester in the depth of the thermal and solutal boundary layers. Also C depreciates with higher values of porous parameter and grows with Δ.
3. Figs.4a-4c are nanoparticle volume fraction (ϕ) and variable parameter (B). B decays the momentum boundary layer thickness at -1.0, 1.0. Also B leads to a reduction in the θ and C distributions. ϕ increases the thermal conductivity and hence enhances the momentum boundary layer thickness at η (-1.0,0) and decays in the flow region(0,1.0). ϕ decreases θ decays in thermal boundary layers while C grows in Eg-Cu nanofluid.
4. Figs.5a-5c are space / temperature dependent heat source parameters (A11 & B11). *u* decelerates in the flow region (-1.0,0) and enhances in (0,1.0) with increase in the strength of A11. *u* grows with higher values of B11. A11, B11 presence of heat is absorbed in the boundary layer which leads to a depreciation in θ & C (A11) grows with rise in B11.
5. Fig.6a-6c are thermal radiation parameter (Rd) and Eckert number (Ec). Higher the Ec larger the magnitude of *u*. θ enhances and C distributions decelerates with increasing Rd and opposite effect is noticed with variation in Ec in the flow region.
6. Fig.7a-7c are asymmetric slips (αo, α1). αo, α1 on the walls demonstrate an increasing tendency in the magnitude of *u*. θ distribution grows and C distribution decays with rising values of αo, α1. Thus the thermal layer turn into strong and solutal layer look good on narrow with higher values of slips (α0, α1).
7. Fig.8a-8c are convective boundary conditions (Bio.Bi1). An increase in Bio on the left wall (η=-1) decays the magnitude of *u* at -1,0 and enhances at 0,1 while the Biot number(Bi1) on the right wall(η=+1) upsurges *u* in magnitude. Increase in Biot number (Bio) leads to a growth in the thickness of the thermal and solutal boundary layers while increase in Bi1 leads to decay in thermal and solutal layers. An augmentation in θ and C with Bio and reduction with Bi1 in the flow region.
8. Fig.9a-9c are Suction parameter(S) and Prandtl number (Pr). *u* enhances in the flow region (-1,0) and reduces in the region (0,1) with increasing S. θ & C grows with rising values of S in the entire flow region. *u* velocity reduces in -1,0 and enhances in (0,1). θ upsurges and C decays with increasing values of Pr in -1, 0 & 0,1.
9. Figs.10a-10c demonstrate the influence of Schmidt number (Sc) and Soret parameter (Sr) on θ and C. Lesser the molecular diffusivity larger the temperature in the entire flow region. The nanoconcentration depreciates in the flow region (-1, 0) and upsurges in the region (0,1.0). The thermal boundary layer becomes thicker with Sc and solutal boundary layers become thinner with Sc. The thickness of thermal and solutal boundary layers decays in the region in (-1,0)and grows in (0,1).with Sr.
10. The effect of chemical reaction parameter (γ) on θ and C in figs.11b-11c. θ & C experiences depreciation in γ>0 and upsurges in γ<0. This is owing to the fact that thickness of the thermal and solutal boundary layers become thinner with values of γ>0 and opposite effect is noticed in γ<0.

11. Fig.12b-12c are activation energy parameter (E1) and temperature difference ratio (δ). From the profiles we find that the thickness of thermal and solutal boundary layers become thicker with rising values of E1 and δ. This results in an upsurges in θ and C with higher values of E1 and δ in the flow region.
12. Figs.13b-13c are Radiation absorption (Q1) and index number (n). The effect of Q1 is to upsurge θ and C. Grows in *n* leads to a growth in θ and C in the entire flow region. This amount to the fact that the thermal and solutal boundary layers becomes thicker with rising values of Q1 and n.
13. The Shear stress(τ) is exhibited in table.3 at the walls η=±1 for different parameters G,M,K,S,Rd,Ec,B,A11,B11,B,ϕ, Δ ,α0,α1,Bio,B11 and Pr. An upsurge in G/ϕ/Rd/A11 grows stress at η=±1 in Eg based Cu nanofluid. Higher the Lorentz force (M)/Suction parameter (S) decays stress at η=+1 & grows at η=-1 in Eg based Cu nanofluid. Increase in B/R/Δ/Ec diminishes the stress at η±1. K reduces stress at η=-1 and enhances at η=+1 in Eg Cu nanofluid. An increase in αo, α1 decays the stress at left wall while at η=1, it upsurge with αo and decays with α1. Upsurge in Biot number (Bi0) leads to a fall in stress at η±=1 while stress grows at η=-1 and diminishes at η=+1 with higher values of Biot number (Bi1). τ with Pr, the thermal diffusivity smaller the stress at the walls.
14. Table 3 are the local Nusselt number (Nu) at the walls η=±1. An upsurge in G/ α0, α1/ Bi0/Pr/Sc/E1/δ/n/Q1/Ec grows Nu at both the walls. Upsurge in M/ K/Δ/ ϕ/B/ A11, B11/ S/Sr/Bi1 diminishes Nu at η=±1. Higher Rd, larger Nu at η=-1 and smaller Nu at η=+1. Nu decays at η=-1 and grows at η=+1 in both γ>0 and γ<0.
15. Sherwood number (Sh) is the rate of mass transfer, at the walls η=±1 in table.3. The values of Sh reduces at η=-1 & upsurges at η=+1 by rising principles of G/ϕ/A11/E1/δ. An increase in M/K/ B/B11/ Bi1/ S/Pr/Sr/Ec grows Sh at η=-1 and falls at η=+1 in Eg based Cu nanofluid. Increase in Δ/α0, α1/Sc/Q1 grows the Sh at η=±1. Higher the Bio/ Rd smaller the Sh at η=±1. Sh enhances at η=-1 and decays at η=+1 in γ>0 while in γ<0 an opposite effect is noticed at η=±1.

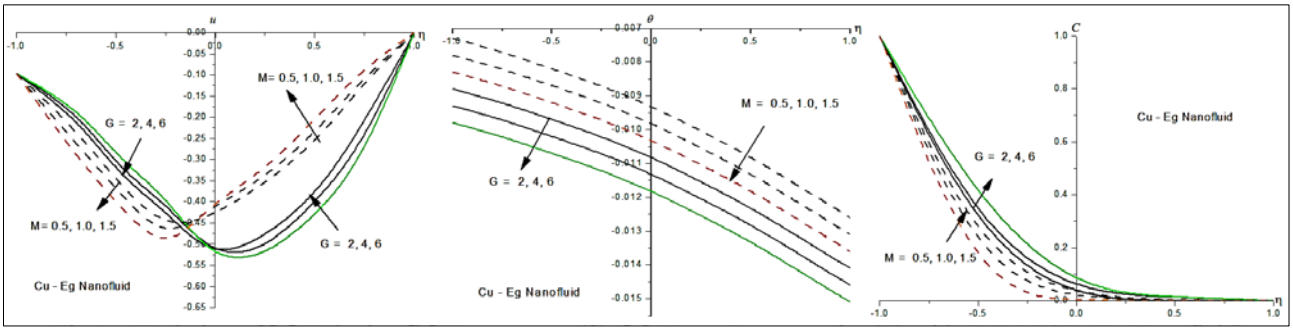

Fig 2: Variation of [a] Velocity, [b] Temperature(θ), [c] Nano-Concentration(C) with G & M (Cu-Eg Nanofluid) Δ=0.2, K=0.2, Rd=0.5, Ec=0.05, A11=0.1, B11=0.2, ϕ=0.05, B=0.2, α1=0.2, α0=0.1, Bi$_0$=1, Bi$_f$=2, S=0.1, Pr=0.71, Sr=0.5, Sc=0.24, γ=0.5, E1=0.2, δ=0.01, Q1=0.25, n=0.2

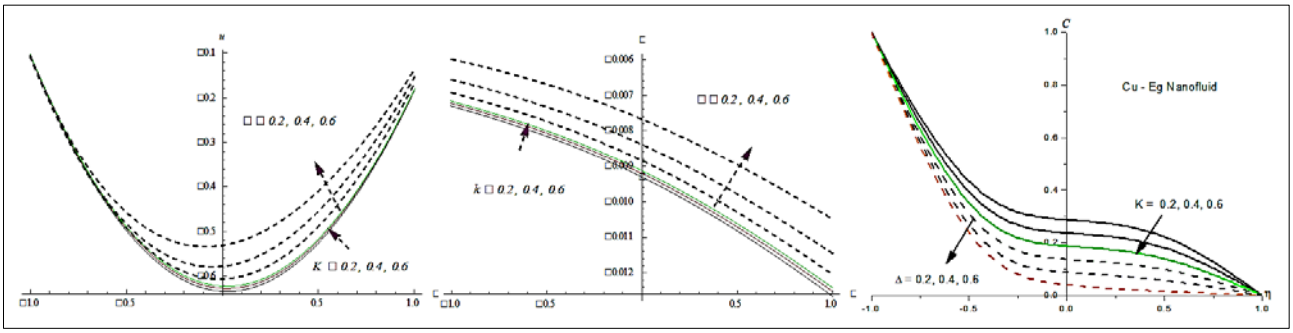

Fig 3: Variation of [a] Velocity, [b] Temperature(θ), [c] Nano-Concentration(C) with K & Δ (Cu-Eg Nanofluid)

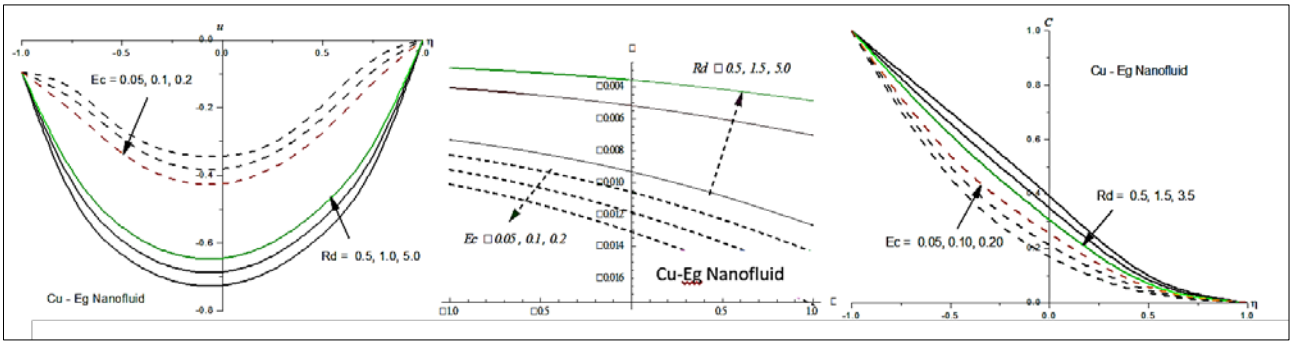

Fig 4: Variation of [a] Velocity, [b] Temperature (θ), [c] Nano-Concentration(C) with Rd & Ec (Cu-Eg Nanofluid)

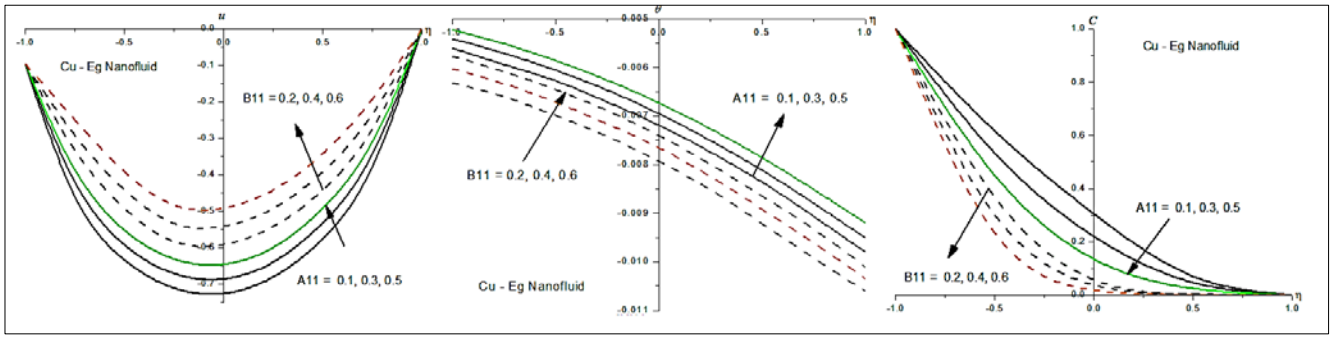

Fig 6: Variation of [a] Velocity, [b] Temperature(θ), [c] Nano-Concentration(C) with ϕ & B (Cu-Eg Nanofluid)

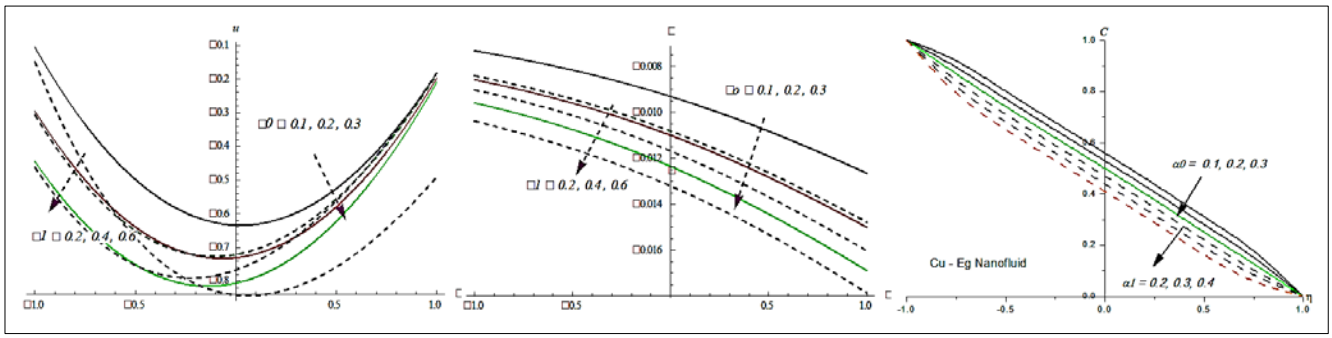

Fig 7: Variation of [a] Velocity, [b] Temperature(θ), [c] Nano-Concentration(C) with α1 & α_0 (Cu-Eg Nanofluid)

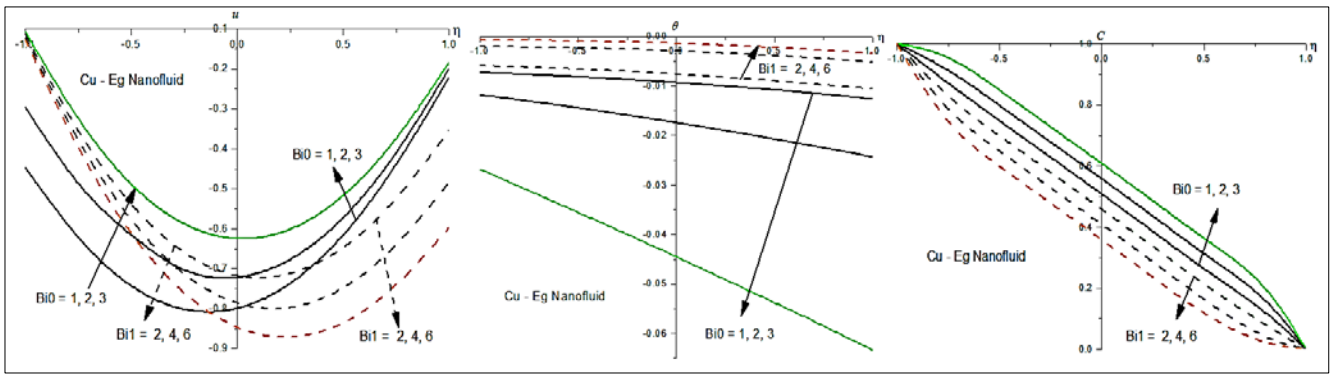

Fig 8: Variation of [a] Velocity, [b] Temperature(θ), [c] Nano-Concentration(C) with Bi_0 & Bi_1 (Cu-Eg Nanofluid)

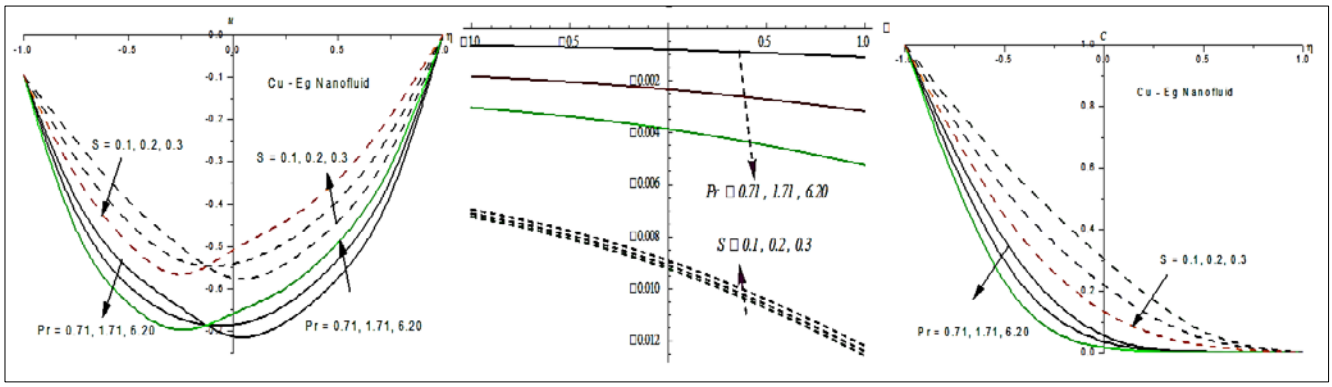

Fig 9: Variation of [a] Velocity, [b] Temperature(θ), [c] Nano-Concentration(C) with Pr & S (Cu-Eg Nanofluid)

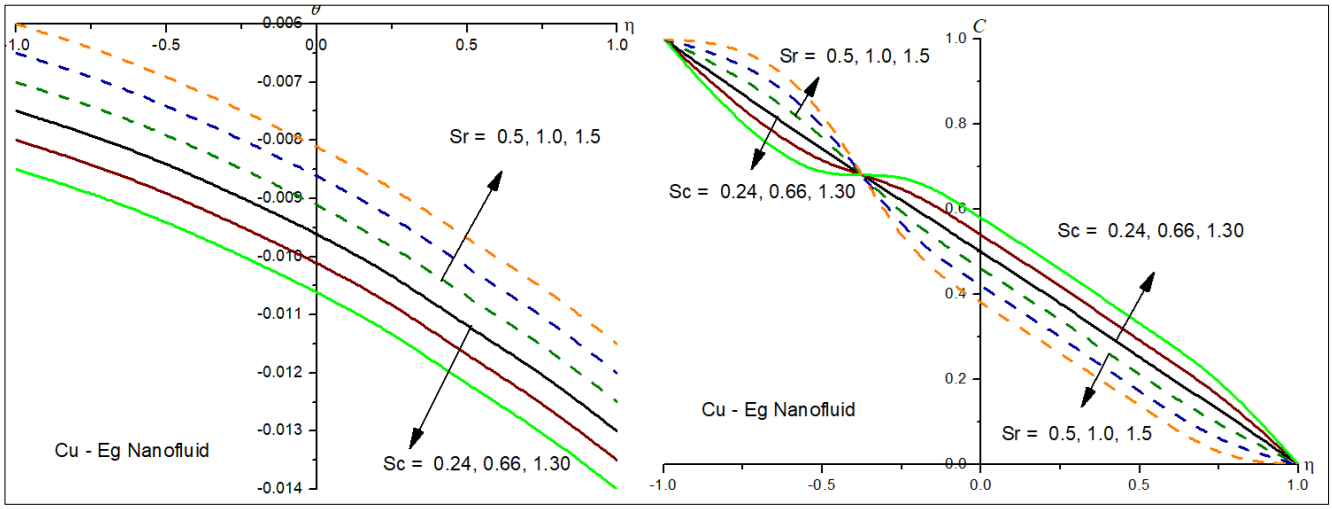

Fig 10: Variation of [a] Temperature (θ), [b] Nano-Concentration(C) with Sc & Sr (Cu-Eg Nanofluid)

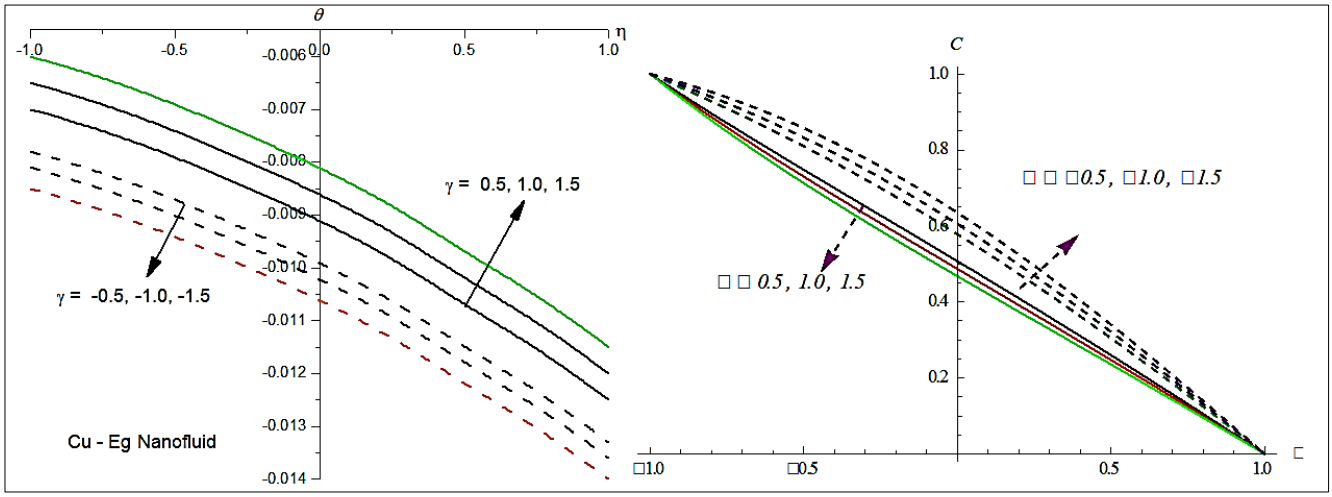

Fig 11: Variation of [a] Temperature (θ), [b] Nano-Concentration(C) with γ (Cu-Eg Nanofluid)

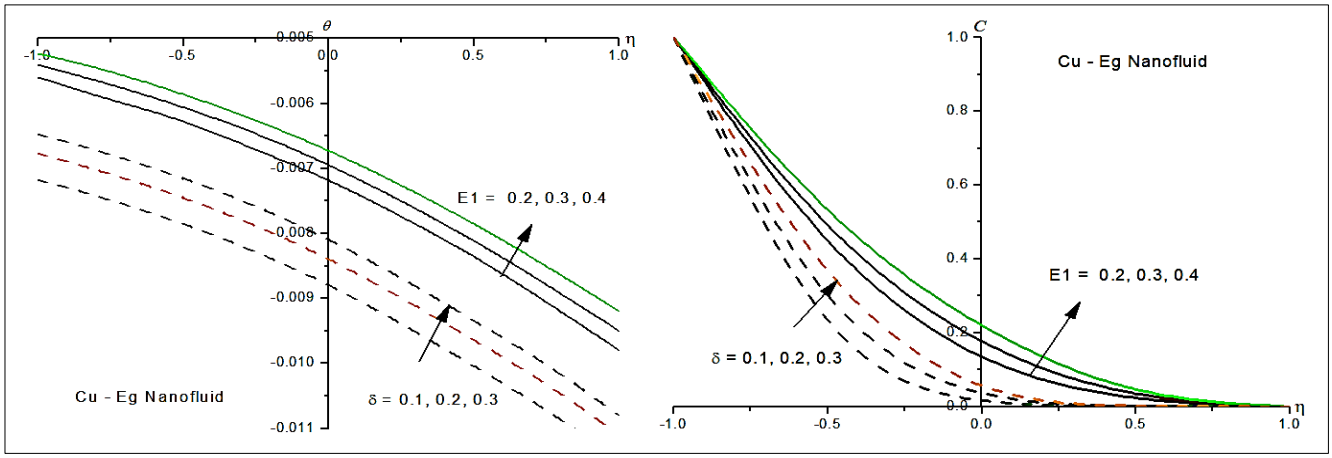

Fig 12: Variation of [a] Temperature (θ), [b] Nano-Concentration(C) with δ & E1 (Cu-Eg Nanofluid)

Table 3: τ ±1(Skin friction), Nu ± 1(Nusselt number) and Sh±1(Sherwood number) at η=±1

Parameter		τ(-1)	τ(+1)	Nu(-1)	Nu(+1)	Sh(-1)	Sh(+1)
G	2	-1.05292	0.914314	0.00149484	0.00388044	0.530345	0.533396
	4	-1.05481	0.916246	0.00149796	0.0038885	0.530164	0.533592
	6	-1.05671	0.918186	0.00150109	0.0038966	0.529981	0.533789
M	0.5	-1.10916	0.862577	0.00147898	0.0038558	0.551647	0.509683
	1	-1.15527	0.809755	0.00145603	0.00381153	0.573466	0.486967
	1.5	-1.17966	0.747541	0.00142837	0.00375405	0.597966	0.463297
K	0.2	-1.05292	0.914314	0.00149484	0.00388044	0.530345	0.533396
	0.4	-1.04368	0.906014	0.00147919	0.00383976	0.531279	0.53243
	0.6	-1.03641	0.899491	0.0014669	0.00380782	0.532014	0.53167

Δ	0.1	-1.07315	0.835067	0.00141713	0.00369411	0.55514	0.506339
	0.2	-1.08687	0.764558	0.00134195	0.0035117	0.579834	0.481289
	0.3	-1.06305	0.680771	0.00122498	0.00321688	0.608394	0.454634
B	0.2	-1.10992	0.862785	0.00147401	0.00384296	0.551563	0.509752
	0.4	-1.16074	0.813041	0.00144698	0.00378803	0.572927	0.487437
	0.6	-1.20716	0.763294	0.00141302	0.00371423	0.595452	0.465389
ϕ	0.05	-1.05292	0.914314	0.00149484	0.00388044	0.530345	0.533396
	0.1	-1.05513	0.921486	0.00146733	0.00386749	0.529892	0.534021
	0.12	-1.05622	0.927226	0.00143978	0.00385075	0.52957	0.534497
Rd	0.5	-1.05292	0.914314	0.00149484	0.00388044	0.530345	0.533396
	1.5	-1.05371	0.91527	0.000576266	0.00149586	0.530256	0.533561
	5	-1.0539	0.915499	0.000356317	0.000924911	0.530234	0.533601
Ec	0.1	-1.11242	0.865065	0.00166442	0.00435909	0.55134	0.509974
	0.2	-1.16529	0.816444	0.00182093	0.00481059	0.572554	0.48778
	0.3	-1.21385	0.767428	0.00195089	0.00519953	0.594943	0.465821
A11	0.1	-1.05292	0.914314	0.00149484	0.00388044	0.530345	0.533396
	0.3	-1.05297	0.914364	0.00144664	0.00375561	0.530341	0.533405
	0.5	-1.053	0.914411	0.00140074	0.00363671	0.530336	0.533413
B11	0.3	-1.11261	0.865237	0.00147697	0.00385071	0.551313	0.510004
	0.5	-1.16569	0.81673	0.00145161	0.00380032	0.572497	0.487836
	1	-1.21448	0.767765	0.00141724	0.00372582	0.594855	0.465895
α0	0.1	-1.05292	0.914314	0.00149484	0.00388044	0.530345	0.533396
	0.2	-0.952083	0.990892	0.00175318	0.00460254	0.503433	0.547418
	0.3	-0.872489	1.05131	0.00196019	0.00518078	0.482196	0.558483
α1	0.2	-0.98803	0.930473	0.00171956	0.00453335	0.524768	0.522637
	0.3	-0.905657	0.91214	0.00184532	0.00491628	0.52746	0.507412
	0.4	-1.48283	0.682803	0.00212238	0.00548334	0.559549	0.518449
Bi0	1	-1.05292	0.914314	0.00149484	0.00388044	0.530345	0.533396
	2	-1.05258	0.913734	0.00301642	0.0053987	0.530314	0.53339
	3	-1.05128	0.911577	0.00868028	0.0110502	0.530198	0.533369
Bi_1	2	-1.11337	0.865821	0.000656611	0.00303697	0.55137	0.510006
	3	-1.16694	0.817444	0.000237073	0.00259717	0.57258	0.487832
	4	-1.21599	0.768398	5.99996E-05	0.0023859	0.594951	0.465883
S	0.1	-1.11261	0.865236	0.00147811	0.00385362	0.551313	0.510004
	0.2	-1.16569	0.816728	0.00145367	0.00380555	0.572497	0.487835
	0.3	-1.21448	0.767763	0.00142181	0.00373743	0.594856	0.465895
Sc	0.24	----	----	0.00153683	0.00401861	0.534073	0.529555
	0.66	----	----	0.0015388	0.00402306	0.603443	0.582943
	1.3	----	----	0.00154081	0.00402752	0.691525	0.641188
Sr	0.5	----	----	0.00153681	0.00401856	0.53438	0.529331
	1	----	----	0.0015368	0.00401853	0.53447	0.529228
	1.5	----	----	0.00153679	0.00401851	0.534561	0.529125
γ	0.5	----	----	0.00153683	0.00401861	0.534073	0.529555
	1	----	----	0.00153364	0.00401013	0.590505	0.502787
	1.5	----	----	0.00153065	0.00400218	0.644606	0.477975
	-0.5	----	----	0.00154796	0.00404813	0.346894	0.624682
	-1	----	----	0.00155214	0.00405922	0.27976	0.661103
	-1.5	----	----	0.00155675	0.00407143	0.207461	0.70163
Q1	0.5	----	----	0.00153683	0.00401861	0.534073	0.529555
	1	----	----	0.00158891	0.00416851	0.534076	0.529558
	1.5	----	----	0.00163057	0.00428843	0.534078	0.529566
E1	0.2	----	----	0.00153683	0.00401861	0.534073	0.529555
	0.3	----	----	0.00153816	0.00402213	0.511058	0.540732
	0.4	----	----	0.00153915	0.00402478	0.493845	0.549187
δ	0.1	----	----	0.00153682	0.00401859	0.534214	0.529476
	0.2	----	----	0.00153683	0.00401862	0.534048	0.529569
	0.3	----	----	0.00153685	0.00401866	0.533806	0.529703
n	0.2	----	----	0.00153682	0.00401858	0.534249	0.529456
	0.4	----	----	0.00153685	0.00401859	0.534208	0.529479
	0.6	----	----	0.00153689	0.0040186	0.534169	0.529501
Pr	0.71	-1.0541	0.915736	0.000129048	0.000335103	0.530212	0.533641
	1.71	-1.05389	0.91548	0.000374199	0.000971453	0.530236	0.533597
	6.2	-1.05368	0.915225	0.000619182	0.00160737	0.53026	0.533553

6. Conclusions

The influence of activity energy, variable viscosity, solar radiation, and dissipation on the convective warmth and mass flow of an Eg-based Cu with asymmetric slips & convective limits at lack of irregular heating elements. The nonlinear, mixed problems were solve by the Finite-element approach using quadratic interpolation function. The results of the above review are:

1. Grows in G upsurges *u*, θ and C in η=±1. τ and Nu grow at η=±1with rising values of G. Sh diminishes by η = - 1 & upsurges by η = + 1 with G.
2. M smaller with *u*, θ and larger C. τ and Sh decays by η = - 1 and downwards by η = + 1. Nu decays at η=±1 with superior values of M.
3. K & Δ smaller *u*, θ. C upsurges with K and grows with Δ. Nu decay among upsurges in K & Δ. τ upsurges by η = - 1 and by η = + 1, it upsurges with K & diminishes with Δ with K and Δ. Sh grows at left wall with K and Δ and at η=+1, it enhances at η=-1, reduces at η=+1.
4. An upwards in suction(S) enhances velocity, reduces temperature and concentration. Stress and Sh enhance at η=+1 and reduce at η=-1. Nu decays at η=±1 with S.
5. The velocity, temperature reduces with Rd and upsurge with higher values of Eckert Number in the flow region. The nanoconcentration enhances with Rd and decays with Ec. Stress increase and Sh reduces with Rd. Nu enhances at η=-1 and decays at η=+1 with Rd. Nu enhances at η=±1 with Ec. Stress and Sh upsurges at η=-1 and decays At η=+1 with rising values of Ec.
6. Increase in space/temperature dependent heat source (A11, B11) decays temperature. C enhances with A11 and reduces with B11 η=±1. *u* enhances with B11 in the entire flow region. τ upsurges by η = - 1 with A11, B11 by η = + 1,τ grows with A11, decays with B11. Nu depreciates with A11 and B11 at η=±1, while Sh enhances with A11 and enhances with B11 at η=-1 and at η=+1, Sh upsurges with A11, diminishes with B11.
7. Grow in ϕ upsurges *u*, C and diminishes θ. τ grows and Nu decays with upsurge in ϕ. Sh diminishes at η=-1 and upwards at η=+1 with ϕ.
8. Higher B, smaller *u*, θ and C in η=±1. Nu decays with B. τ and Sh upsurges at η=-1 and decays at η=+1 with rising values of B.
9. Lesser the molecular diffusivity, larger θ and smaller C in η±1. Nu and Sh upsurge with higher values of Sc on η=±1
10. Higher the thermo-diffusion (Sr) smaller temperature and nanoconcentration. Nu reduces at both walls. Sh upsurges at η=-1 and decays at η=+1 with rising values of Sr.
11. Temperature and nanoconcentration upsurge with E1, δ, n and Q1.Nu enhances with E1, δ, Q1, n at η=±1. Sh diminishes at η=-1 and upsurges at η=+1 with E1, δ while it enhances at both the walls with n/Q1.
12. Higher the inertia and boundary effects smaller *u*, θ and larger C in η±=1. Nu decays and Sh grows with Δ. τ upsurges by η = - 1 and decays by η = + 1 with grows in Δ.
13. Enlarge in asymmetric slips (αo,α1) consequences in an augmentation in velocity and temperature η=±1 and concentration decays with higher values of (αo,α1). Increase in αo and α1 enhances Nu and Sh at both walls. Stress diminishes by η = - 1 and by η = + 1, it upsurges with (αo) and reduces with α1.
14. Increase in Biot numbers (Bio) upsurges temperature and concentration while velocity decays. Velocity enhances, temperature and nanoconcentration decays with upper values of Bi1 η=±1. Stress and Sherwood number decay, Nu grows with increase in Bio. Nu decays with Bi1. Stress and Sherwood number enhance at η=-1 and reduces at η=+1 with rising values of Bi1.

7. References

1. Abbasbandy S, Shirzadi A. A new application of the homotopy analysis method: solving the *Sturm–Liouville* problems. Communications in Nonlinear Science and Numerical Simulation. 2011;16:112–126.
2. Abu-Nada E, Masoud Z, Hijazi A. Natural convection heat transfer enhancement in horizontal concentric annuli using nanofluids. International Communications in Heat and Mass Transfer. 2008;35(5):657–665. doi:10.1016/j.icheatmasstransfer.2007.11.004
3. Abu-Nada E. Effects of variable viscosity and thermal conductivity of CuO-water nanofluid on heat transfer enhancement in natural convection: mathematical model and simulation. Journal of Heat Transfer. 2010;132(5):052401. doi:10.1115/1.4000440
4. Eegunjobi AS, Makinde DO. Second law analysis for MHD permeable channel flow with variable electrical conductivity and asymmetric Navier slips. Open Physics. 2015;13:100–110. doi:10.1515/phys-2015-0014
5. Alam MS, Ahammad MU. Effects of variable chemical reaction and variable electric conductivity on free convective heat and mass transfer flow along an inclined stretching sheet with variable heat and mass fluxes under the influence of Dufour and Soret effects. Nonlinear Analysis: Modelling and Control. 2011;16:1–16.
6. Ali ME. The effect of variable viscosity on mixed convection heat transfer along a vertical moving surface. International Journal of Thermal Sciences. 2006;45:60–69.
7. Arrhenius S. Activation energy and the Arrhenius equation. In: Introductory Chemistry, 1st Canadian Edition. opentextbc.ca; 2017. Archived from the original on July 8, 2017. Retrieved April 5, 2018.
8. Anghel M, Takhar HS, Pop I. Dufour and Soret effects on free convection boundary layer over a vertical surface embedded in a porous medium. Heat and Mass Transfer. 2000;43:1265–1274.
9. Awais M, Hayat T, Ali A, Irum S. Velocity, thermal and concentration slip effects on a magnetohydrodynamic nanofluid flow. Alexandria Engineering Journal. 2016;55:2107–2114. doi:10.1016/j.aej.2016.06.027
10. Barletta A, Celli M, Magyari E, Zanchini E. Buoyancy MHD flows in a vertical channel: the levitation regime. Heat and Mass Transfer. 2007;44:1005–1013.

11. Barletta A, Magyari E, Keller B. Dual mixed convection flows in a vertical channel. International Journal of Heat and Mass Transfer. 2005;48:4835–4845.
12. Boundary layer flow through a porous medium over a vertical plate. Journal of Computational and Applied Research in Mechanical Engineering. 2016;5:111–126.
13. Cebeci T, Khattab AA, LaMont R. Combined natural and forced convection in vertical ducts. Proceedings of the 7th International Heat Transfer Conference. 1982;3:419–424.
14. Cheng KS, Hi JR. Steady, two-dimensional natural convection in rectangular enclosures with differently heated walls. Transactions of the ASME. 1987;109:400.
15. Choi SUS, Eastman JA. Enhancing thermal conductivity of fluids with nanoparticles. Materials Science. 1995;231:99–105.
16. Choi SUS. Enhancing thermal conductivity of fluid with nanoparticles. In: Siginer DA, Wang HP, editors. Developments and Applications of Non-Newtonian Flows. FED 231/MD 66. 1995. p. 99–105.
17. Choi SUS, Zhang ZG, Yu W, Lockwood FE, Grulke EA. Anomalous thermal conductivity enhancement in nanotube suspensions. Applied Physics Letters. 2001;79:2252–2254.
18. Das SK, Choi SUS, Yu W, Pradeep T. Nanofluids: Science and Technology. New Jersey: Wiley; 2007.
19. Datta N, Jana RN. Effect of wall conductance on hydromagnetic convection of a radiation gas in a vertical channel. International Journal of Heat and Mass Transfer. 1974;19:1015–1019.
20. Devasena Y. Effect of non-linear thermal radiation and activation energy on hydromagnetic convective heat and mass transfer flow of nanofluid in vertical channel with Brownian motion and thermophoresis in the presence of irregular heat sources. World Journal of Engineering Research and Technology. 2023;9(2):xx–xx. Available from: www.wjert.org
21. Ellahi R, Hayat T, Mahomed FM, Asghar S. Effects of slip on the non-linear flows of a third grade fluid. Nonlinear Analysis: Real World Applications. 2010;11(1):139–146.
22. Falade J. Entropy generation analysis for porous channel flow with asymmetric slip and thermal boundary conditions. Chemical and Process Engineering Research. 2016;46:1–7. Available from: www.iiste.org
23. Gill WN, Del Casal A. A theoretical investigation of natural convection effects in forced horizontal flows. AIChE Journal. 1962;8:513–518.
24. Hayat T, Safdar A, Awais M, Mesloub S. Soret and Dufour effects for three-dimensional flow in a viscoelastic fluid over a stretching surface. International Journal of Heat and Mass Transfer. 2012;55:2129–2136.
25. Hayat T, Farooq MA, Javeda T, Sajid M. Partial slip effects on the flow and heat transfer characteristics in a third grade fluid. Nonlinear Analysis: Real World Applications. 2009;10:745–755.
26. Hayat T, Hina S, Ali N. Simultaneous effects of slip and heat transfer on the peristaltic flow. Communications in Nonlinear Science and Numerical Simulation. 2010;15:1526–1537.
27. Hayat T, Hussain Q, Qureshi MU, Ali N, Awatif, Hendi A. Influence of slip condition on the peristaltic transport in an asymmetric channel with heat transfer: An exact solution. International Journal for Numerical Methods in Fluids. 2011;63:1944–1959.
28. Kathyani G, Venkata Subrahmanyam P. Effect of dissipation on HD convective heat and mass transfer flow of thermally radiating nanofluid in vertical channel with activation energy and irregular heat sources. MukthShabd Journal. 2023;12(3):433–441.
29. Kiran T, Kumar P, Srinivasa Rao, Shamshuddin MD. Effect of thermal radiation on non-Darcy hydromagnetic convective heat and mass transfer flow of a water–SWCNT's and MWCNT's nanofluids in a cylindrical annulus with thermo-diffusion and chemical reaction. International Journal of Modern Physics B. 2024;38(1):2450011. https://doi.org/10.1142/S0217979224500115.
30. Kumar BR, Sivaraj R, Benazir J. Chemically reacting MHD free convective flow over a vertical cone with variable electric conductivity. International Journal of Pure and Applied Mathematics. 2015;5:821–828.
31. Lalramngaihzuali H, Prasada Rao DRV. Numerical study of MHD convective heat transfer flow of ethylene glycol based SWCNT and MWCNT nanofluids in cylindrical annulus with variable viscosity, activation energy. International Journal of Novel Research and Development. 2024;9(3):1–10.
32. Lesnic D, Ingham DB, Pop I, Storr C. Free convection boundary layer flow above a nearly horizontal surface in a porous medium with Newtonian heating. Heat and Mass Transfer. 2004;40:665–672.
33. Makinde OD, Mabood F, Khan WA, Tshehla MS. MHD flow of a variable viscosity nanofluid over a radially stretching convective surface with radiative heat. Journal of Molecular Liquids. 2016;219:624–630. http://dx.doi.org/10.1016/j.molliq.2016.03.078.
34. Merkin JH. Natural convection boundary-layer flow on a vertical surface with Newtonian heating. International Journal of Heat and Fluid Flow. 1994;15:392–398.
35. Mondal RK, Hossain MA, Rana BMJ, Ahmmed SF. Radiation and chemical reaction effects on free convection and mass transfer flow of dissipative fluid past an infinite vertical plate through a porous medium. Elixir International Journal. 2015;84:523–530.
36. Muralidhar P. Effect of chemical reaction and thermo diffusion on convective heat and mass transfer flow of viscous fluid through a porous medium in a vertical channel [PhD thesis]. Vishakhapatnam: Andhra University; 2012.
37. Muthu P, Tesfahun B. Fluid flow in an asymmetric channel. Tamkang Journal of Mathematics. 2011;42(2):149–162. doi:10.5556/j.tkjm.42.2011.149-162.
38. Nagasasikala M. Effect of activation energy on convective heat and mass transfer flow of dissipative nanofluid in vertical channel with Brownian motion and thermophoresis in the presence of irregular heat sources. World Journal of Engineering Research and Technology. 2023;9(2):1–10.

39. Satya Narayana K, Ramakrishna GN. Effect of variable viscosity, activation energy and irregular heat sources on convective heat and mass transfer flow of nanofluid in a channel with Brownian motion and thermophoresis. World Journal of Engineering Research and Technology. 2023;9(2):1–10.
40. Ostrach S. Combined natural and forced convection laminar flow and heat transfer of fluid with and without heat sources in channels with linearly varying wall temperature. NACA Technical Note. 1954;3141:1–20.
41. Ozotop HF, Abu-nada E. Numerical study of natural convection in partially heated rectangular enclosures filled with nanofluids. International Journal of Heat and Fluid Flow. 2004;29:2395–2401.
42. Prakash J, Prasad PD, Kumar RVMS, Varma SVK. Diffusion-Thermo effects on MHD free convective radiative and chemically reactive flows. Journal reference incomplete; 2016.
43. Raju MC, Reddy NA, Varma SVK. Analytical study of MHD free convective dissipative boundary layer flow past a porous vertical surface in presence of thermal radiation, chemical reaction and constant suction. Ain Shams Engineering Journal. 2014;5:1361–1369. https://doi.org/10.1016/j.asej.2014.07.005.
44. Rashidi MM, Domairry G, Dinarvand S. Approximate solutions for the Burger and regularized long wave equations by means of the homotopy analysis method. Communications in Nonlinear Science and Numerical Simulation. 2009;14:708–717.
45. Rao BM, Reddy GV. Soret and Dufour effects on hydro-magnetic heat and mass transfer over a vertical plate in a porous medium with a convective surface boundary condition and chemical reaction. International Journal of Engineering Research and Applications. 2012;2(4):56–76.
46. Singh V, Shweta A. Flow and heat transfer of Maxwell fluid with variable viscosity and thermal conductivity over an exponentially stretching sheet. American Journal of Fluid Dynamics. 2013;3(4):87–95.
47. Tiwari A. Activation energy impacts on hydromagnetic convective heat transfer flow of nanofluid past a surface of vertical wavy with variable properties. International Journal of Computer Applications. 2023;184(50):1–6.
48. Umamaheswar M, Raju MC, Varma SVK, Gireeshkumar J. Numerical investigation of MHD free convection flow of a non-Newtonian fluid past an impulsively started vertical plate in the presence of thermal diffusion and radiation absorption. Alexandria Engineering Journal. 2016;55:2005–2014. https://doi.org/10.1016/j.aej.2016.07.014.
49. Vajravelu K, Prasad KV, Chiu-on N. Unsteady convective boundary layer flow of a viscous fluid at a vertical surface with variable fluid properties. Nonlinear Analysis: Real World Applications. 2013;14:455–464.
50. Vedavathi N, Ramakrishna K, Reddy KJ. Radiation and mass transfer effects on unsteady MHD convective flow past an infinite vertical plate with Dufour and Soret effects. Ain Shams Engineering Journal. 2014;6:363–371. https://doi.org/10.1016/j.asej.2014.09.009.